

Electronic supplementary information

Functionalizing graphene oxide framework membranes with sulfonic acid groups for superior aqueous mixture separation

Guang Yang,^{ab} Zongli Xie,^{*b} Marlene Cran,^a Derrick Ng,^b Christopher D. Easton,^b Mingmei Ding,^c Hang Xu^c and Stephen Gray^{*a}

^a *Institute for Sustainable Industries and Liveable Cities, Victoria University, PO Box 14428, Melbourne, VIC 8001, Australia.*

^b *CSIRO Manufacturing, Private bag 10, Clayton South, VIC 3169, Australia.*

^c *College of Environmental Science, Hohai University, 1 Xikang Road, Nanjing 210098, China.*

Corresponding author emails: stephen.gray@vu.edu.au; zongli.xie@csiro.au

Experimental Section

Materials

Nylon (polyamide) microfiltration membranes provided by Sterlitech with nominal inner pore size of 0.22 μm were used as the substrates. Commercial GO produced by Hummers method was obtained from XFNANO CO. Ltd (diameter from 500 nm to 5 μm and thickness from 0.8 to 1.2 nm, >99.0%). NaCl (>99.0%), Na₂SO₄ (>99.0%), MgCl₂ (>99.0%), MgSO₄ (>99.0%), HCl (32%), methanol (>99.5%), ethanol (>99.7%) and iso-propanol (>99.7%) were supplied by Merck KGaA. CaCl₂ (>99.0%) and KCl (>99.0%) were obtained from Thermo Fisher Scientific. Iso-butanol (>99.7%), SSA (70.0%) and SA (>99.0%) were purchased from Sigma-Aldrich. All the chemicals in this research were of analytical grade and used as received without further purification. Milli-Q deionised water (18.1 M Ω · cm at 25 °C) was used to prepare the aqueous GO, SSA, solvent and saline solutions.

Membrane preparation

The GOF-SSA membranes were prepared by vacuum filtering diluted GO and SSA aqueous mixture through the nylon substrate (nylon shows strong adhesion with GO, possibly resulted from the strong hydrogen bonds between the amino or oxygen containing groups with the hydroxyl and carboxyl groups of GO, and the water contact angle of nylon substrate is $68 \pm 3^\circ$ as shown in Fig. S23). 0.005 mg mL⁻¹ GO aqueous suspension was realized by dispersing an amount of predetermined GO powders in Milli-Q water under sonicating of 50 Hz at room temperature. Then SSA was added into 20 mL of GO suspension in a flask. The weight ratio between GO and SSA was fixed at 1:10 and the amount of GO deposited on the substrate was varied depending on the volume of GO dispersion. Before pressure was applied, the GO-SSA mixture was placed in the filtration flask for 2 min to obtain good contact between the nylon surface and the GO-SSA mixture. Then, the pressure of the vacuum side was on and maintained at 133.3 Pa until no liquid flow to the vacuum side was observed. A further extension (5-30 min depending on the amount of GO) of the vacuum state was required to dry the deposited GO layer and form a thin film on the substrate. Then, a specific volume of SSA (equivalent to half the weight of the GO deposited) was filtered through the membrane followed by another filtration of 1 mL of HCl (5 mol L⁻¹). When the HCl filtration was completed, the membrane was placed in an oven at 80 °C for 1 hour. Finally, the as-prepared membrane was immersed in deionized water to remove unreacted SSA as well as HCl, dried in the ambient environment and then stored for later performance tests and characterizations. The same fabrication method was applied for the GOF-SA membrane using SA instead. The control GO membrane and precursor GOF-SSA were obtained by simply filtering the GO dispersion or GO with SSA solution without HCl and heat treatment.

Pervaporation performance

Performance tests were carried out using a laboratory scale PV unit as described in previous studies (Fig. S22†). To ensure the reproducibility, 3 identical membranes of each type (GO, GOF-SA or GOF-SSA) were used for every performance test, and the average result of the three tests is reported. Error bars shown in figures represent the standard deviation of the results. A membrane was placed in the middle of a PV cell fixed by O-rings. The effective transport area of the membrane is 4.6 cm². Synthetic NaCl solution (3.5 wt%) or equivalent molar concentration of other saline solutions such as KCl, Na₂SO₄, MgCl₂, and MgSO₄ were used as the feed solution for PV desalination and alcohol-water binary mixtures (80 wt% of alcohol and 20 wt% of water) for solvent dehydration. The feed was preheated in a water bath to the required temperature and pumped to the PV cell by a Masterflex® peristaltic pump. The flow rate of the feed was maintained at 50 mL min⁻¹ and the corresponding crossflow feed velocity is 0.064 cm s⁻¹. A K-type thermocouple was installed in the feed chamber to monitor the operating feed temperature. Absolute pressure applied on the permeate side of the membrane cell was maintained at 133.3 Pa using a vacuum pump and the permeate was collected in a dry-ice cold trap. In this study, it was observed that a minimum of 30 min was required to reach membrane performance stability. The performance test was conducted for 4 h whereas the long-term stability test using synthetic seawater containing CaCl₂, MgCl₂, NaCl and KCl, was lasted for 50 h. The corresponding mass concentrations for the main cations were 412 ppm, 1,272 ppm, 10,787 ppm and 397 ppm, respectively. The electrical conductivity of the synthetic seawater was 51.2 mS cm⁻¹ derived using a pre-calibrated Oakton® Con 110 conductivity meter. The water flux (J) was determined from the mass (M) of permeate collected in the cold trap, the effective membrane area (A) and the experimental time (t). The pervaporation desalination performance was evaluated by J and salt rejection (R), which were calculated by the following equations, respectively;

$$J = \frac{M}{A \times t} \quad (1)$$

$$R = \frac{C_f - C_p}{C_f} \times 100\% \quad (2)$$

The salt concentration of the feed was symbolled as C_f . It should be noted that at the end of the performance test, the permeate side of the membrane was immediately flushed with a known amount of deionized water (excluding the membranes for EDS test). The salt amount of this stream was taken into account for the permeate concentration, *i.e.* C_p (mol L^{-1}) was composed of the amount of salts in the permeate plus the amount of salts in the flush and then divided by the liquid volume collected in the permeate side.

For the dehydration of alcohol–water binary mixtures, the same setup and experiment conditions as those of desalination by PV was applied. Alcohol concentration in the permeate side was determined by nuclear magnetic resonance (NMR, Bruker 400 Ultrashield with Icon NMR analysis software). The membrane performance was evaluated by flux as expressed before and separation factor (α);

$$\alpha = \frac{P_W/P_A}{F_W/F_A} \quad (3)$$

P_w and P_A refer to the mass percent of water and alcohol in the permeate side, respectively; F_w and F_A are the respective mass percentages of water and alcohol in the feed.

The relationship between the permeation flux and temperature for pervaporation generally follows the Arrhenius equation;

$$J_i = A_i \exp\left(-\frac{E_a}{RT}\right) \quad (4)$$

where J_i is the permeate flux of the membrane, $\text{kg m}^{-2} \text{h}^{-1}$; A_i is the pre-exponential factor, $\text{kg m}^{-2} \text{h}^{-1}$;

R is the gas constant (8.3145×10^{-3} kJ mol⁻¹ K⁻¹), T is the absolute temperature, K and E_a is the apparent activation energy for the permeates, kJ mol⁻¹; which relies on the activation energy for diffusion as well as the sorption heat. The Arrhenius equation can be transposed to calculate the E_a using $\ln J_i$ vs. $1000/T$ as follows:

$$\ln J_i = \ln A_i - \frac{E_a}{RT} \quad (5)$$

Characterization

Both the surface and cross-section morphologies of the membranes were characterized by scanning electron microscope (SEM, Zeiss Merlin Gemini 2) with an acceleration voltage of 7 kV. The elemental distribution of membranes was investigated by Energy Dispersive Spectrometers (EDS, Oxford Instrument with JED-2300 Analysis Station) equipped on SEM. To confirm the permeation of salts through the membranes, the membranes were subject to EDS without flushing the surface or bottom by deionized water after the performance test, otherwise the membrane was washed for calculation of salt rejection. Membrane samples were coated by sputtering with iridium for SEM and EDS observations. The working distance is 5 mm. The TECNAI 12 transmission electron microscope (TEM) under an accelerating voltage of 200 kV was used to observe the cross-section of the GOF-SSA membrane by producing a thick freestanding GO or GOF membrane sample. The surface roughness of the membranes was characterized by atomic force microscope (AFM, Bruker FastScan atomic force microscope) with Icon scanning head and ultrasharp silicon nitride tips of a typical force constant of 0.4 N/m and a resonant frequency of 70 kHz. Scan size of 10 μ m were performed at 0.7 Hz and 512 data points per scan line. The peak-force set-point, while controlled by the instrument, was typically less than 2 nN. All images were processed, and lines cans obtained using NanoScope Analysis 1.9 software. The surface roughness results are presented and compared in terms of Rq (nm), which is the root mean square average of height deviation taken from the mean image data plane.

The elemental states of the as-fabricated membranes were observed by an X-ray photoelectron spectroscopy (XPS, AXIS-Nova spectrometer) equipped with a monochromated Al K α source at a power of 180 W. Binding energies were referenced to the C1s peak at 284.8 eV. The total pressure in

the main vacuum chamber during analysis was typically between 10^{-9} and 10^{-8} mbar. Survey spectra were acquired at a pass energy of 160 eV. To obtain more detailed information about chemical structure, oxidation states etc., high resolution spectra were recorded from individual peaks at 40 eV. Each specimen was analyzed at an emission angle of 0° as measured from the surface normal. Assuming typical values for the electron attenuation length of relevant photoelectrons the XPS analysis depth (from which 95 % of the detected signal originates) ranges between 5 and 10 nm for a flat surface.

The interlayer spacing of the membranes for both dry and wet state were determined by X-ray diffraction (XRD, Bruker D8) with Cu-K radiation (45kV, 200mA). The samples were scanned over the 2θ range 2° to 70° with a step size of 0.04° and a scan rate of 1 degree per minute. The carbon state of the membrane samples was investigated by Raman spectroscopy (Chameleon He-Ne laser generator with $\lambda=531.6$ nm). The functional structure of fabricated membrane samples was assessed by attenuated total reflectance-Fourier transform infrared (ATR-FTIR) spectroscopy using a Perkin-Elmer Spectrum 2000 FTIR instrument with frequency range from 4000 to 520 cm^{-1} . The hydrophilic properties of membrane samples were assessed by a KSV contact angle meter (CAM200) equipped with an image capturing system. Static contact angles were measured by the sessile drop method. A 6 μL water drop was formed on the levelled surface of the membrane for contact angle measurements. Surface charging behaviors in terms of zeta potential were determined by an electrokinetic analyzer (SurPASS, Anton Paar GmbH, Austria) in the pH range of 3-11. For the above-mentioned characterization, 3 samples of each type (GO, GOF-SA or GOF-SSA) were characterized and the average result was reported. Variation in the results is shown by error ranges that represent the standard deviation.

Supplementary Figures

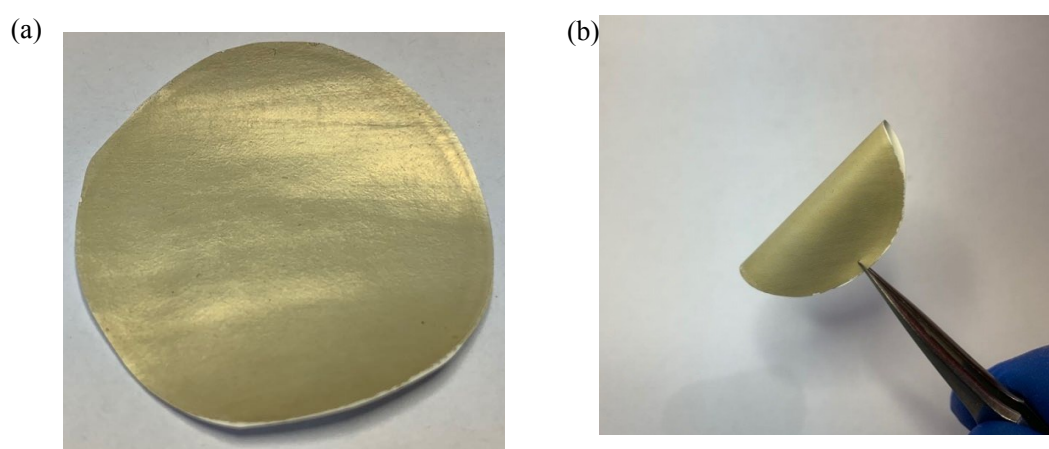


Fig. S1 Optical images of GOF-SSA membrane; (a) surface view and (b) bent state of the GOF-SSA membrane.

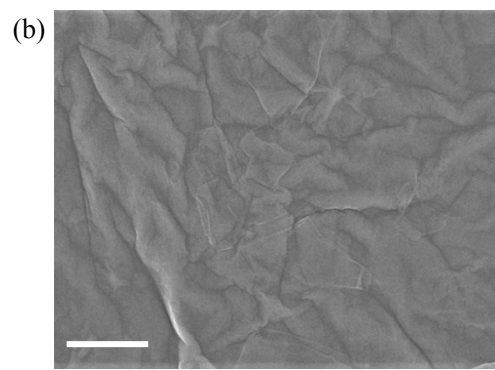
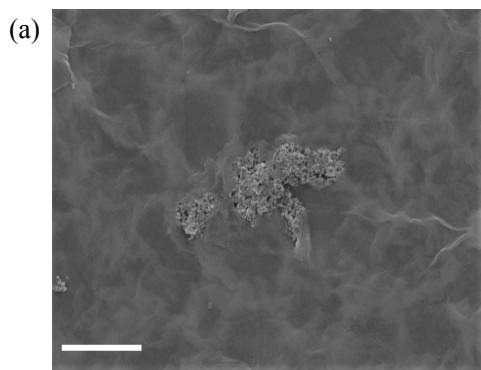


Fig. S2 Observable defects on the GOF-SSA membrane surface (a) using SEM when GOF thickness was less than 50 nm and GOF-SSA surface with clear GO boundaries (b). Scale bar 1 μm .

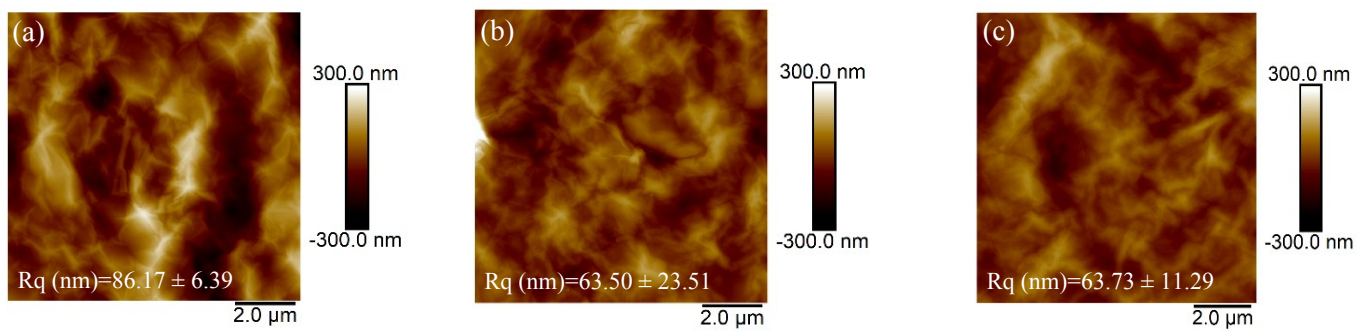


Fig. S3 AFM surface roughness of (a) control GO, (b) GOF-SA and (c) GOF-SSA.

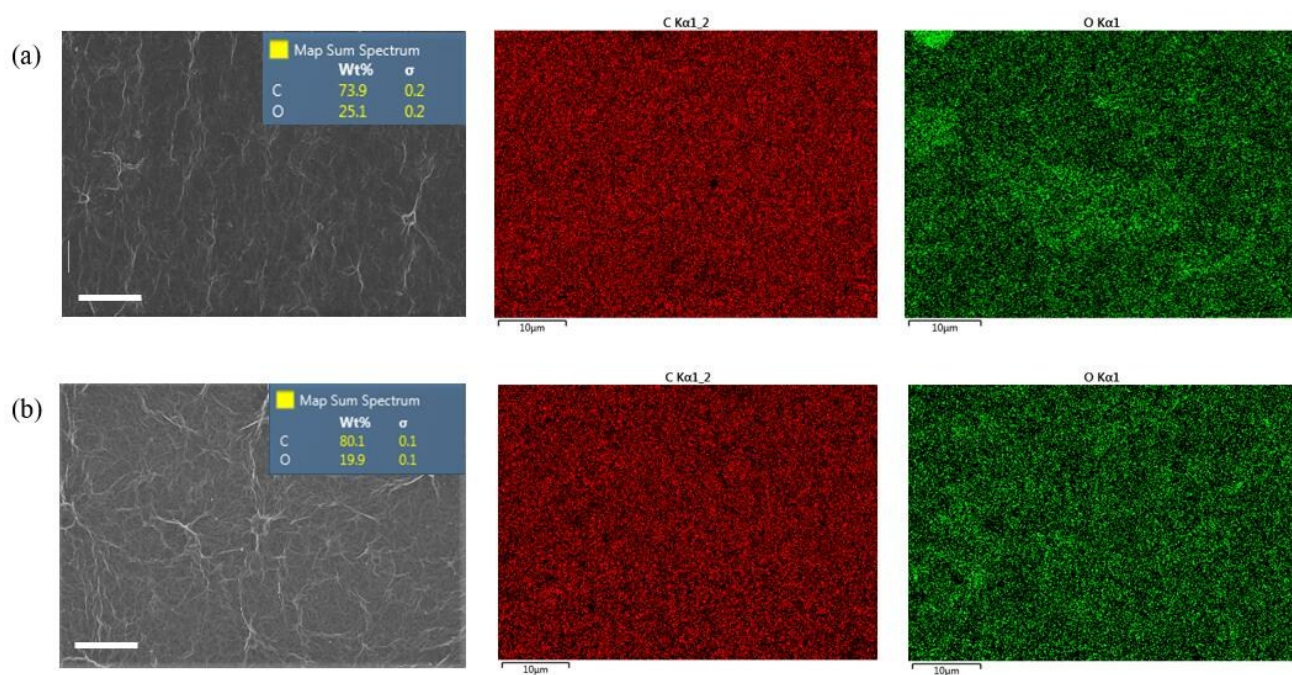


Fig. S4 EDS elemental mapping of the surface of (a) control GO and (b) GOF-SA fragments. Scale bar 10 μ m.

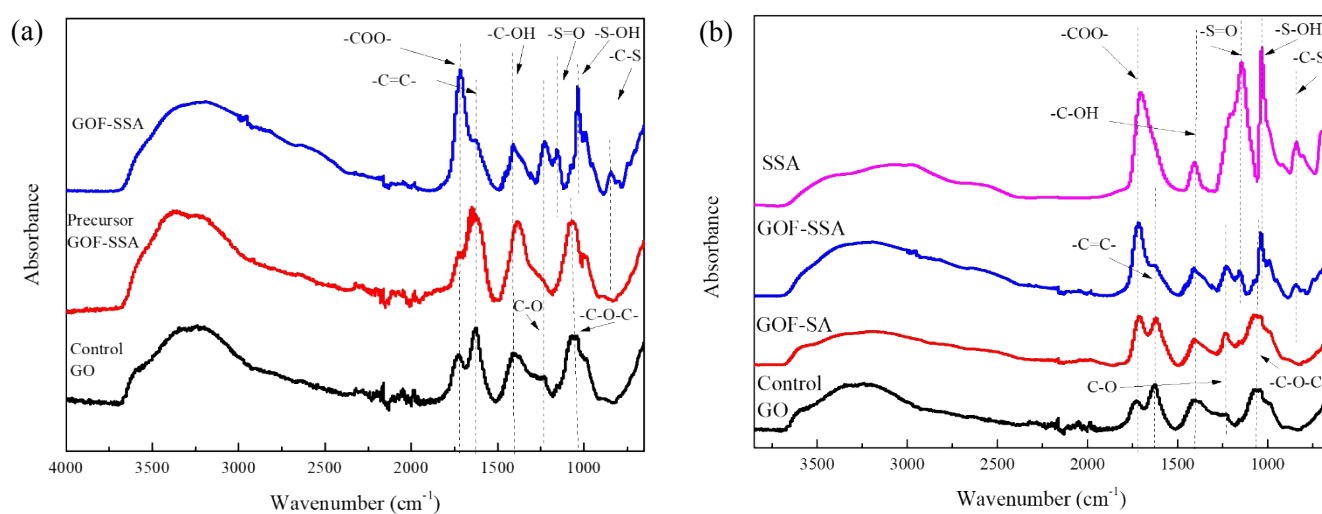


Fig. S5 FTIR results of (a) a comparison between precursor GOF-SSA, control GO and GOF-SSA; (b) comparison between SSA, GOF-SSA, GOF-SA and control GO.

For the control GO membrane, the spectrum shows a series of characteristic peaks of the oxygen-containing groups belonging to the GO nanosheets. Similar to the SSA, a broad peak centered at 3240 cm^{-1} corresponds to the stretching vibrations of C-OH and the intercalated H_2O . Strong peaks at 1725 cm^{-1} , 1617 cm^{-1} , 1352 cm^{-1} , 1220 cm^{-1} and 1045 cm^{-1} are attributed to the C=O stretching vibrations from carboxylic and carbonyl groups, C=C in aromatic rings, C-OH deformation vibrations, C-O-C stretching and breathing vibrations, respectively.

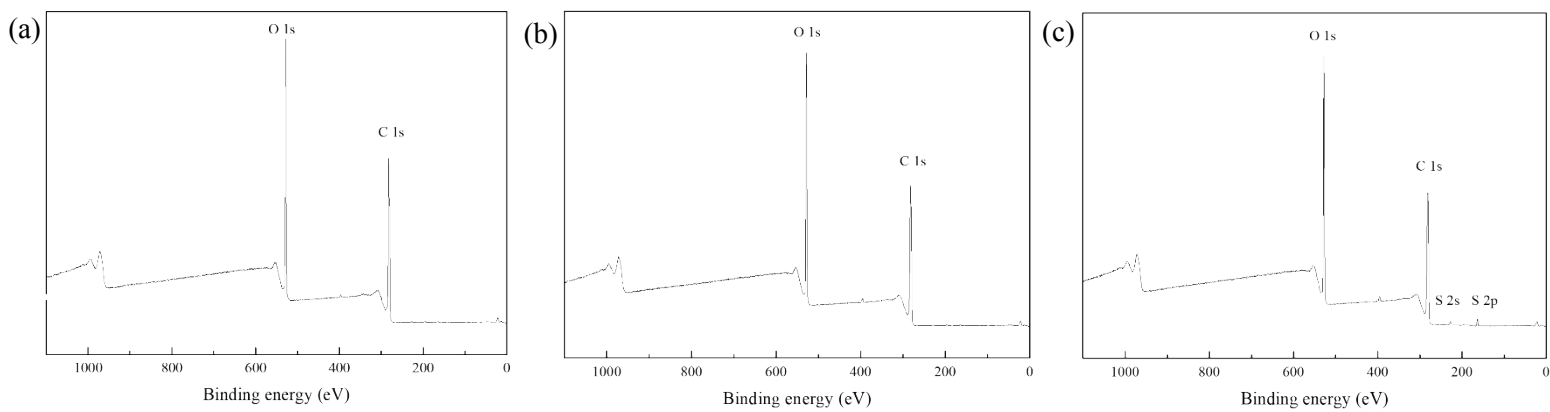


Fig. S6 XPS survey spectra of (a) control GO, (b) GOF-SA and (c) GOF-SSA.

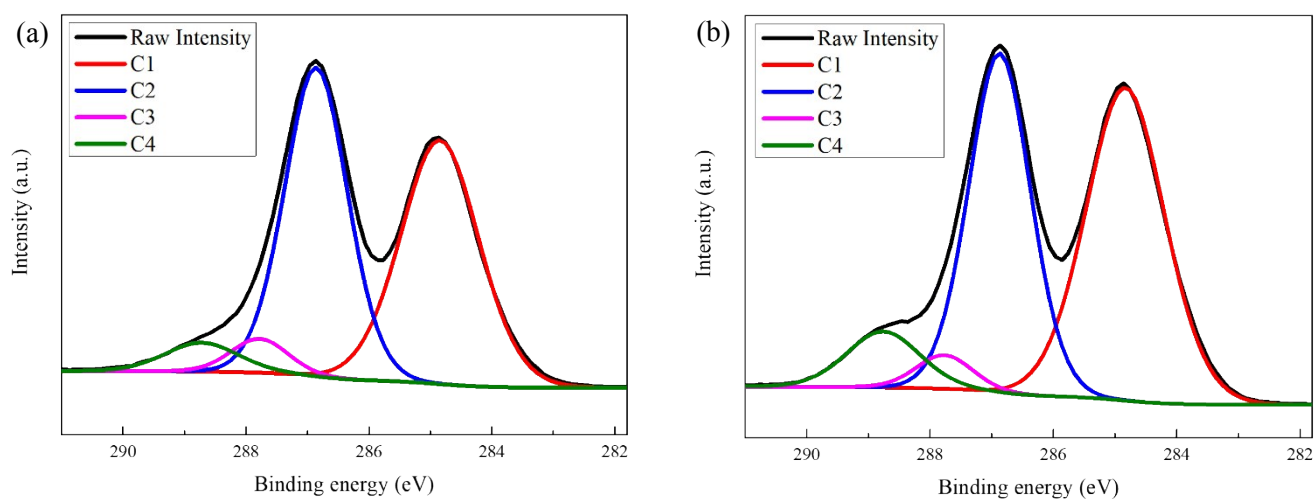


Fig. S7 XPS spectra fitted with a 4-component system of (a) control GO and (b) GOF-SA, where the assignments for the components are as follows: C1: C=C/C-C/C-H/C-S; C2: C-O-C/C-OH; C3: C=O and C4: O-C=O.

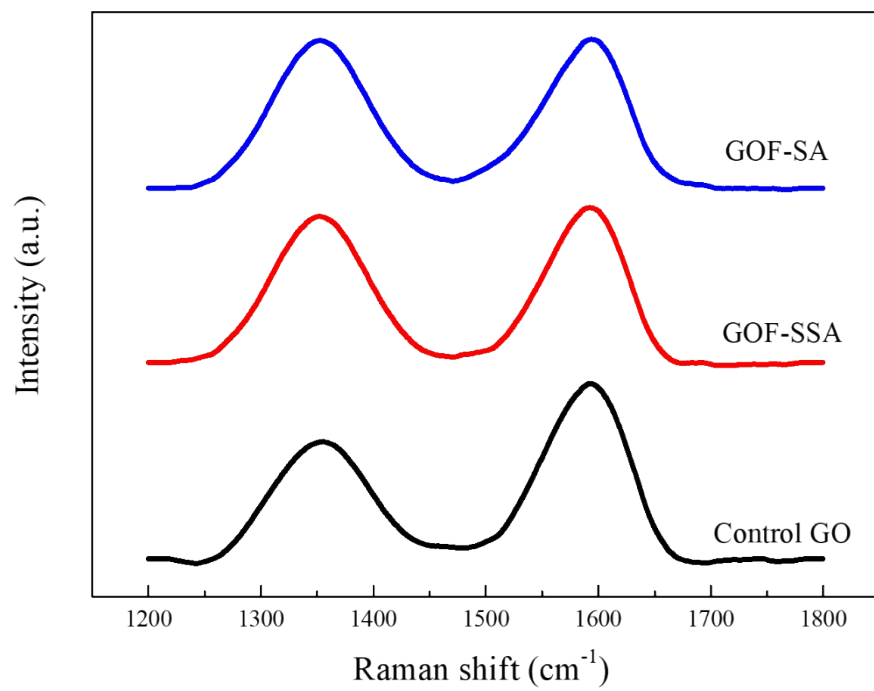


Fig. S8 Raman spectra of control GO, GOF-SSA and GOF-SA.

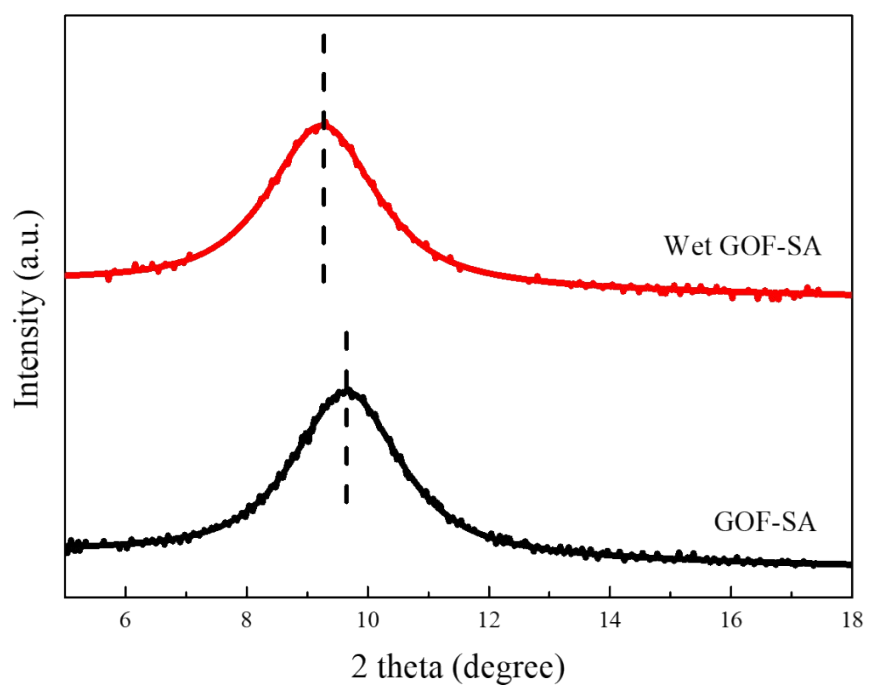


Fig. S9 XRD patterns of GOF-SA before and after wetting in water.

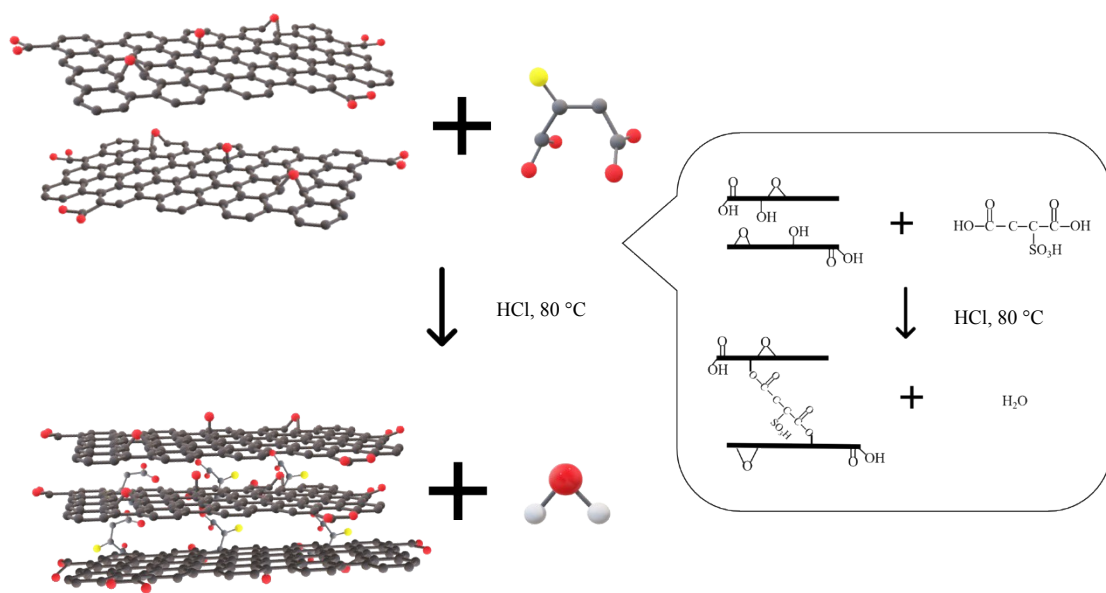


Fig. S10 Proposed aslant linking of SSA with GO nanosheets.

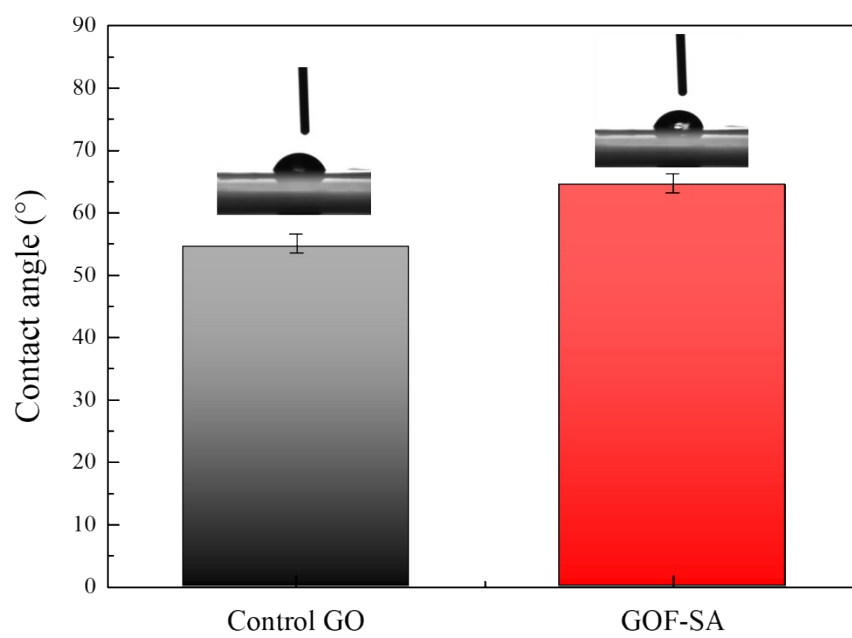


Fig. S11 WCA comparison between control GO and GOF-SA.

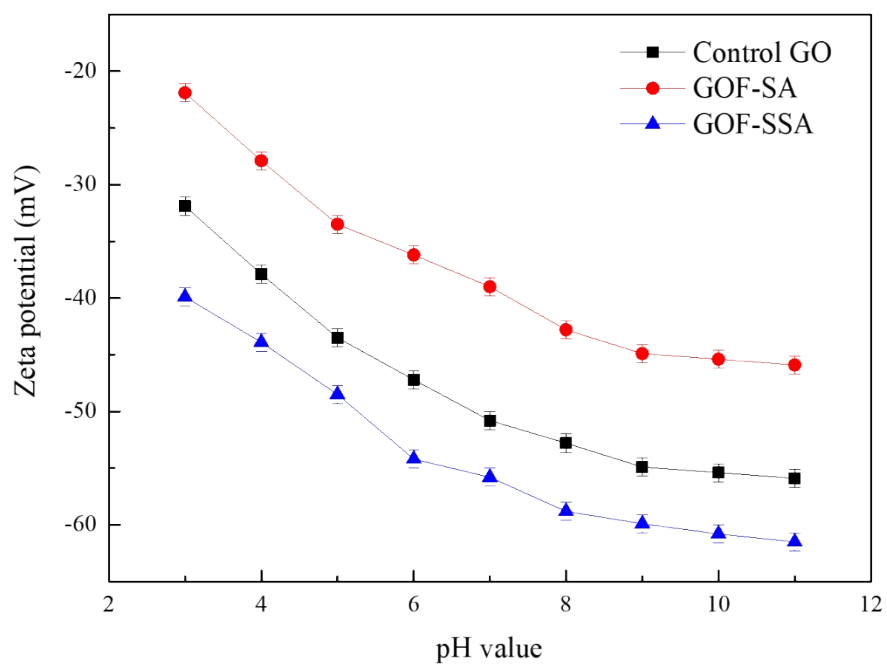


Fig. S12 Zeta-potential of control GO, GOF-SSA and GOF-SA in pH range 3-11.

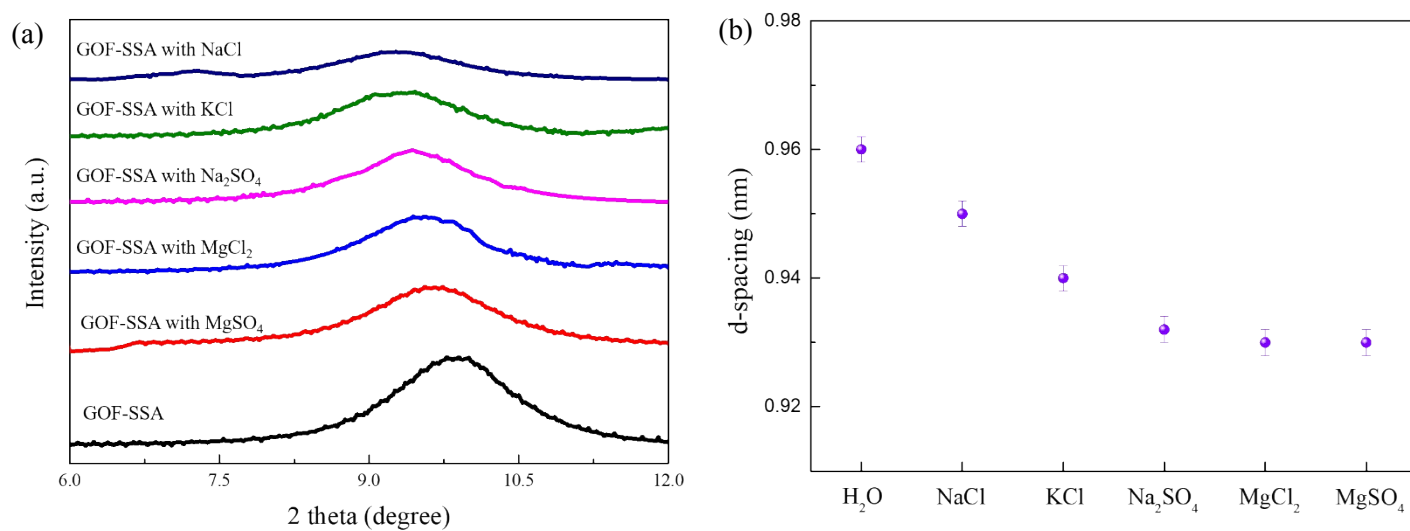


Fig. S13 (a) XRD patterns of GOF-SSA in various saline solution (3.5 wt% NaCl or equivalent molar concentration of KCl, Na₂SO₄, MgCl and MgSO₄, respectively) and (b) corresponding d-spacing value of GOF-SSA in various salt solutions.

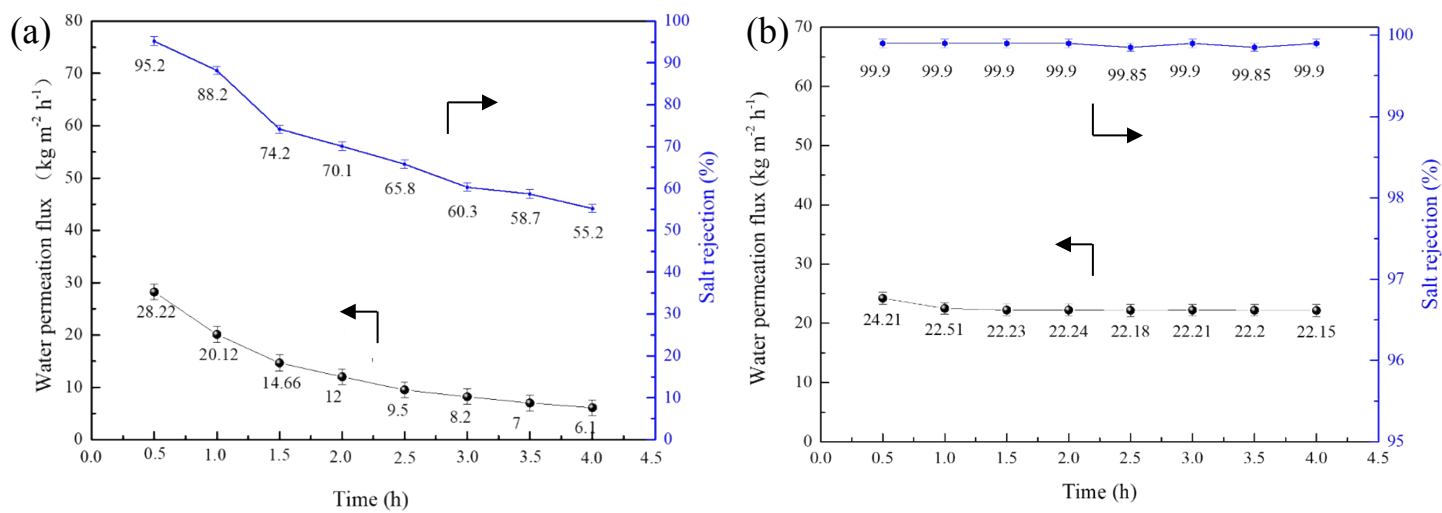
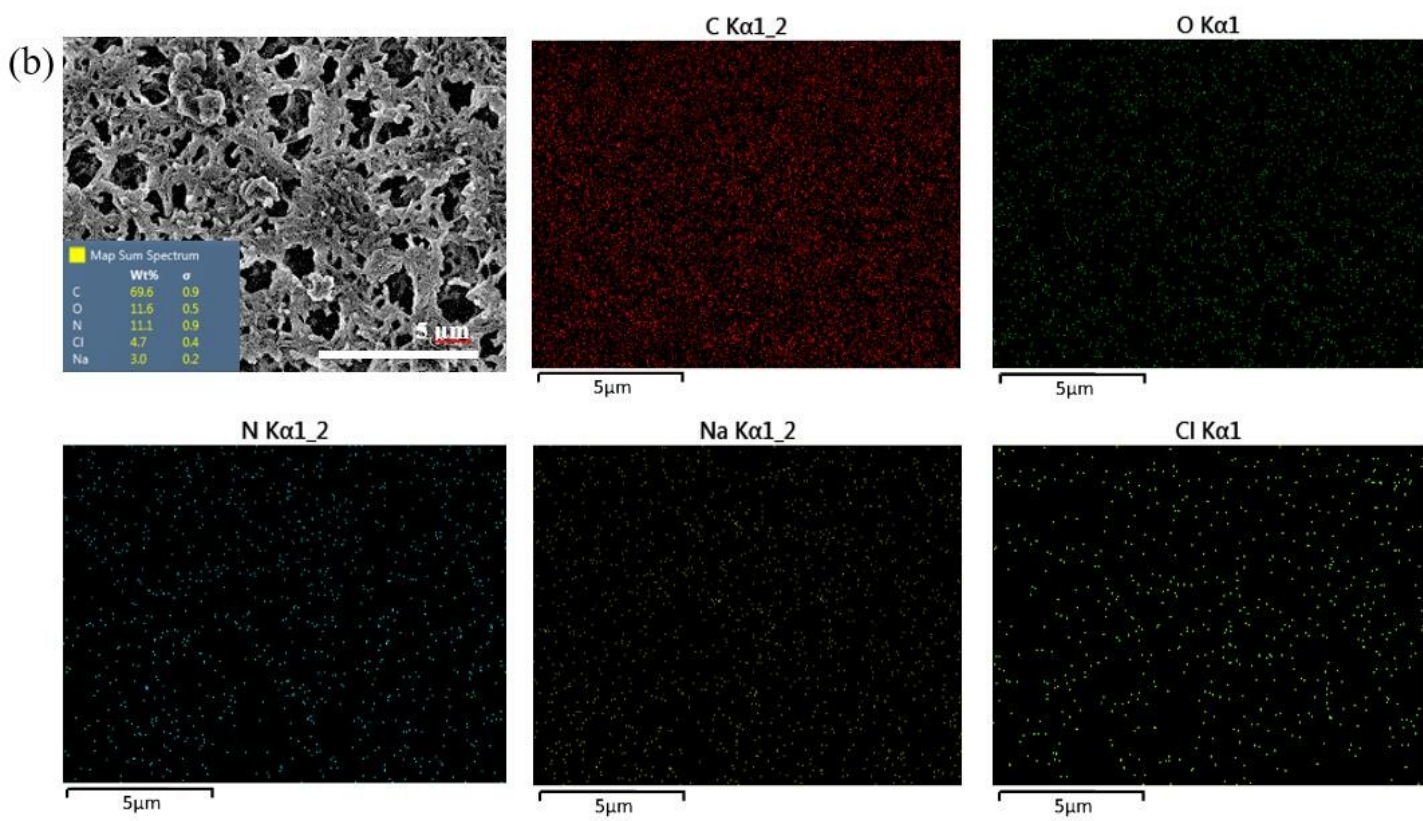
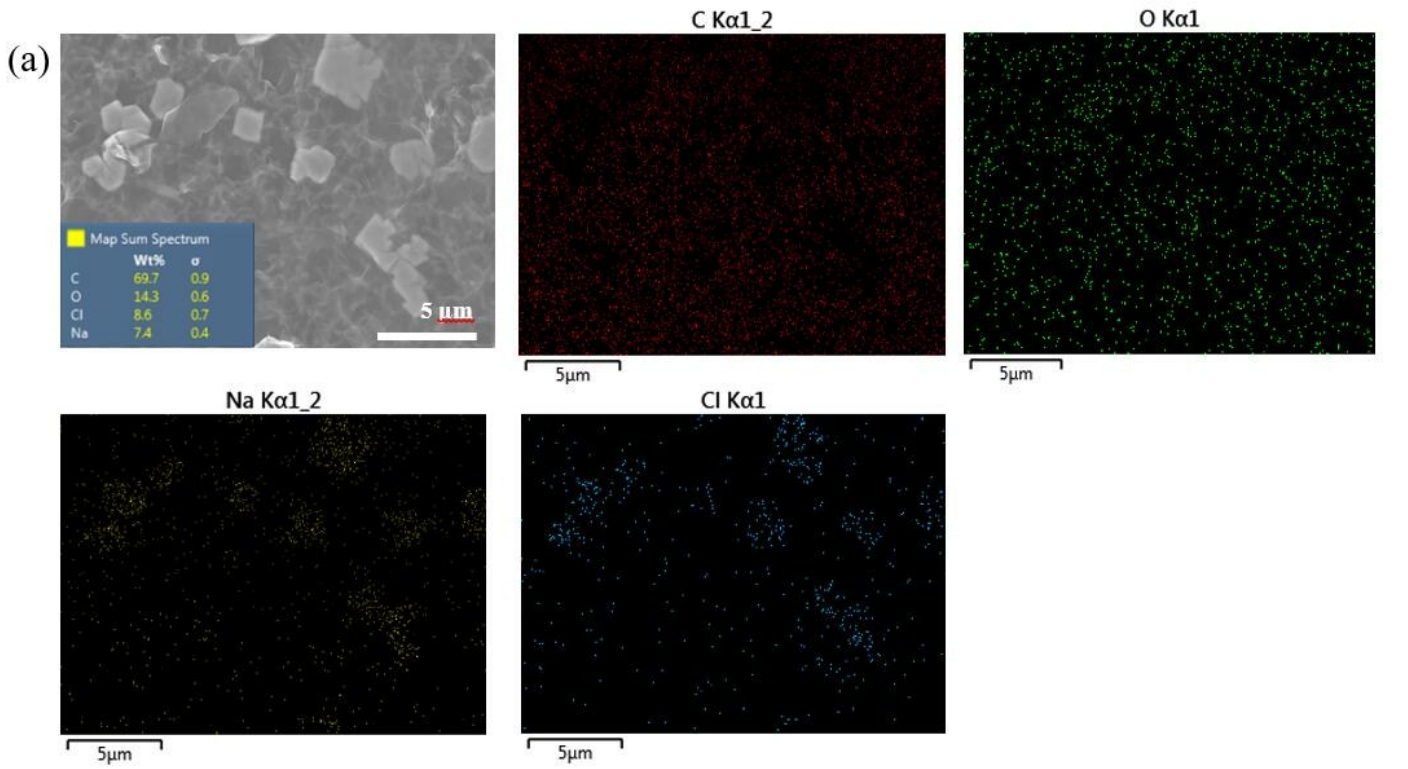


Fig. S14 Performance comparison between (a) control GO and (b) GOF-SSA in 4-hour test (3.5 wt% NaCl as feed, 30 °C of pervaporation temperature, 133.3 Pa of permeate side and sampling every 0.5 h).



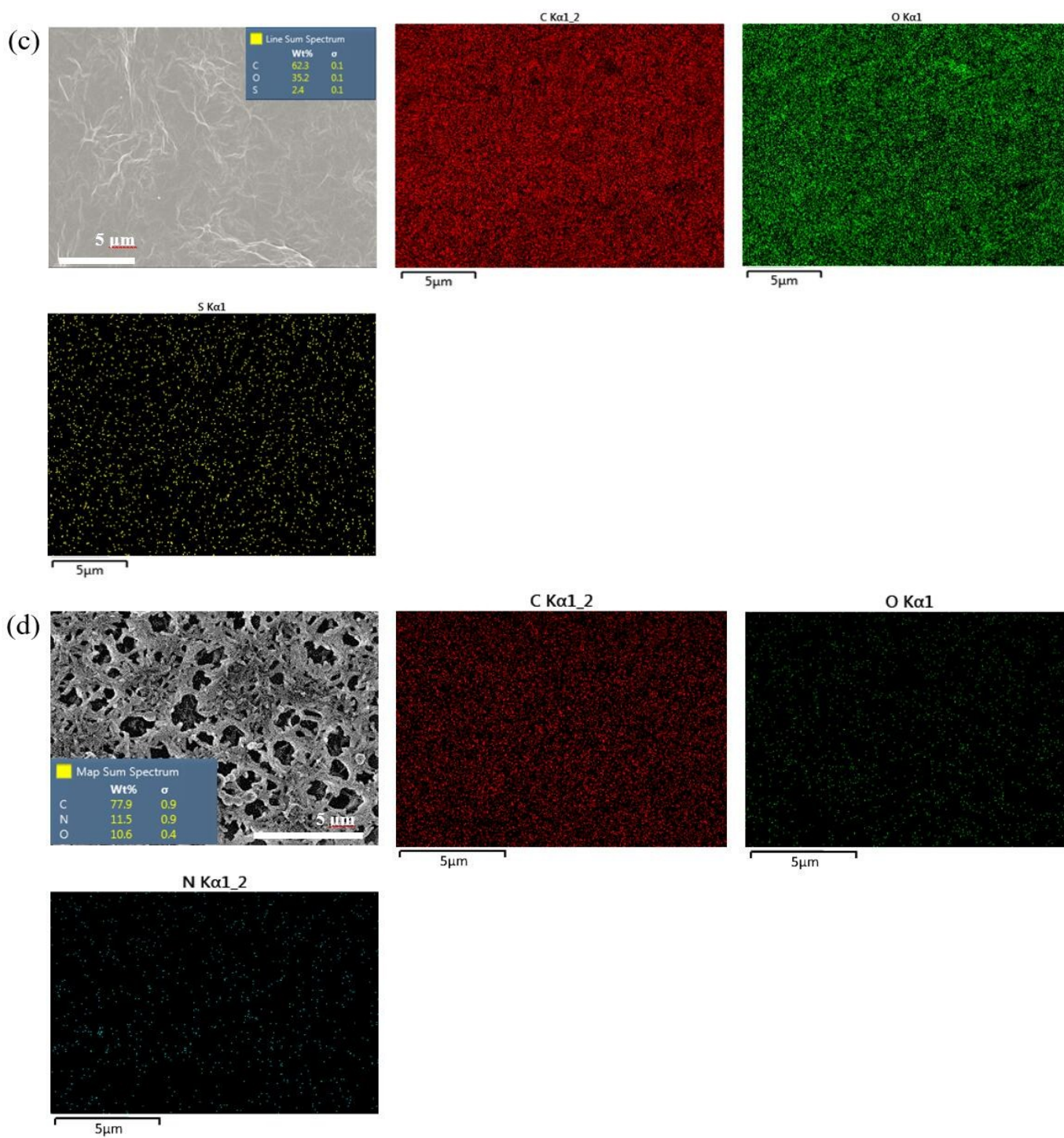


Fig. S15 Surface EDS of control GO after pervaporation test (a); downstream side EDS of control GO

membrane after pervaporation test (b); surface EDS of GOF-SSA after pervaporation test (c); downstream side EDS of GOF-SSA membrane after pervaporation test (d).

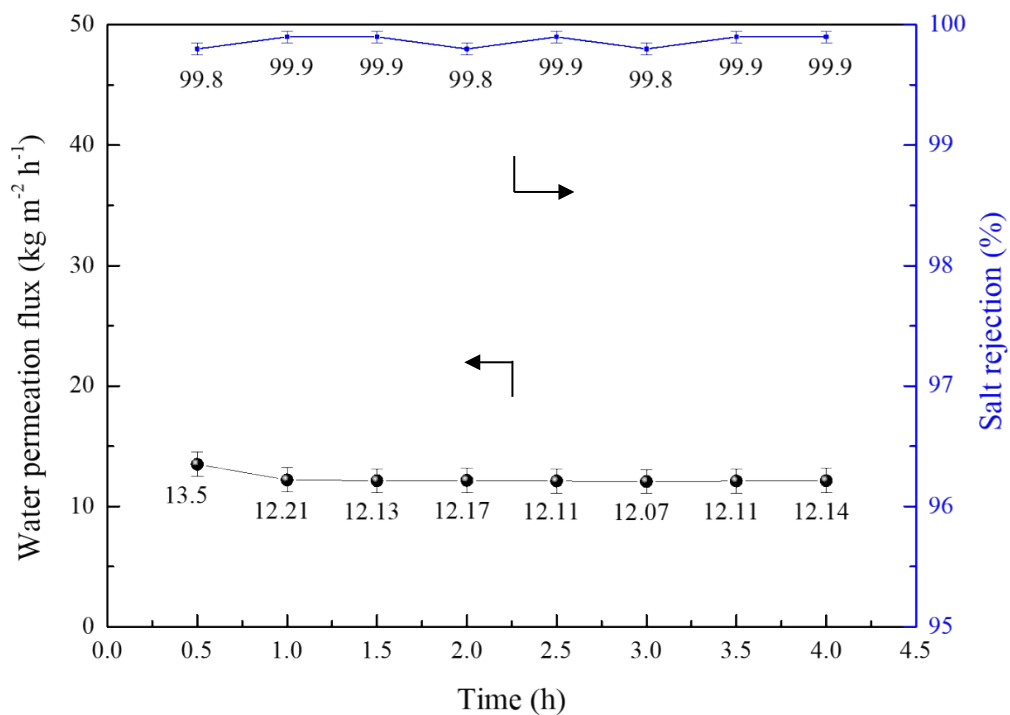


Fig. S16 Desalination performance of GOF-SA using 3.5 wt% NaCl solution as feed with sampling every 0.5 h.

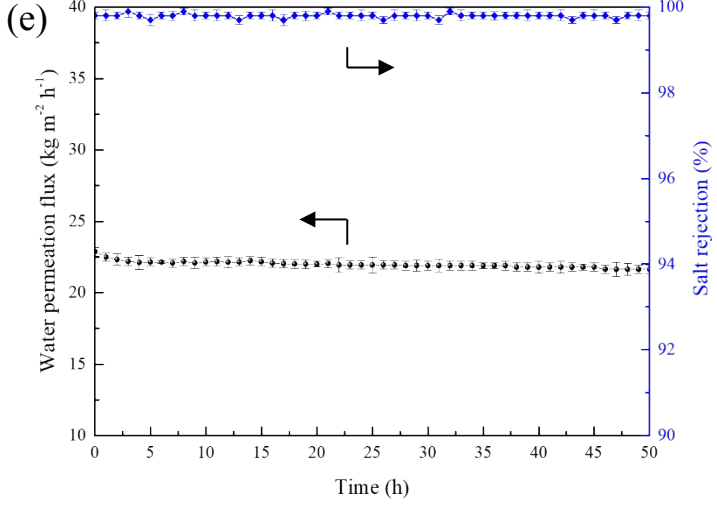
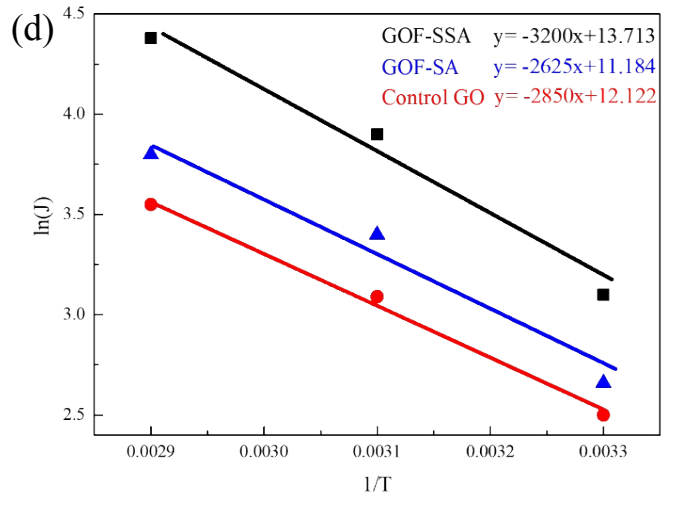
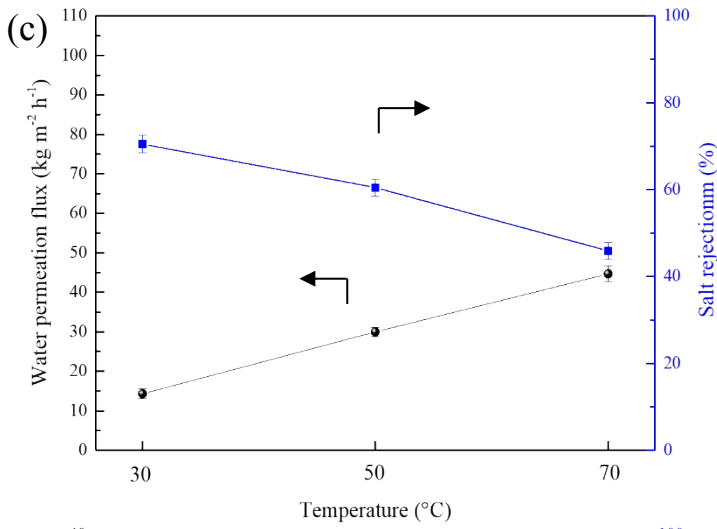
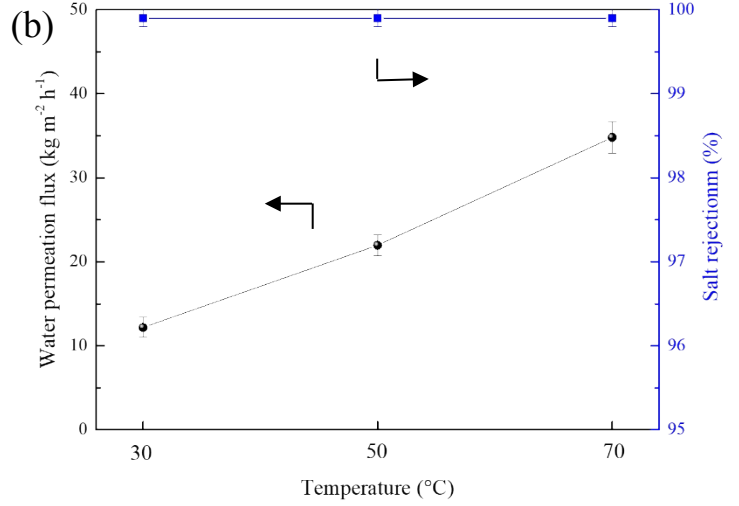
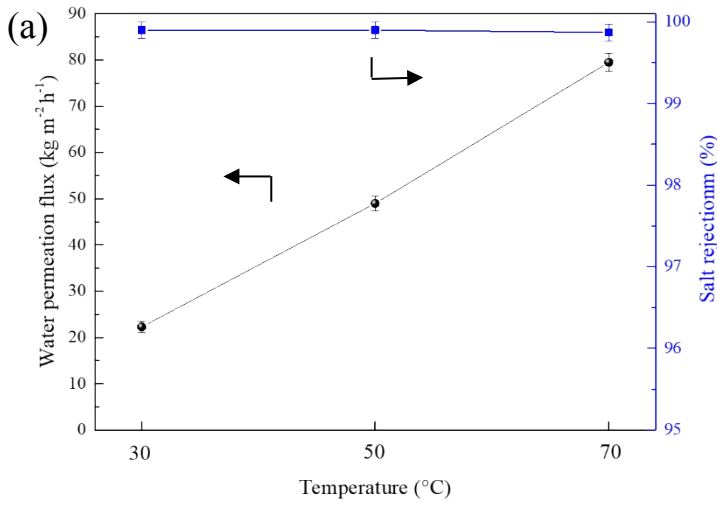


Fig. S17 Pervaporation performance of (a) GOF-SSA, (b) GOF-SA and (c) Control GO at different temperatures using 3.5 wt% NaCl solution as feed. Permeate pressure: 133.3 Pa. (d) the Arrhenius plot of the water flux and feed temperature and (e) Long-term stability test at 30 °C using synthetic seawater. Permeate pressure: 133.3 Pa. Feed flow rate: 50 mL min⁻¹.

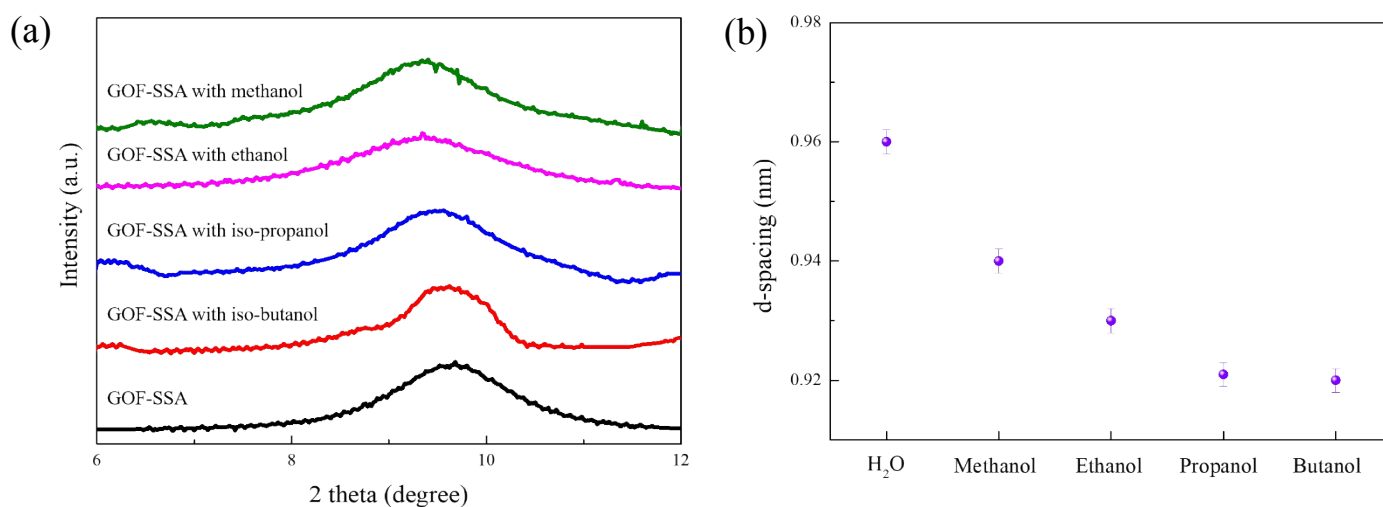


Fig. S18 (a) XRD patterns of GOF-SSA in various water-alcohol solution (80 wt% alcohol and 20 wt% water) and (b) corresponding d-spacing value of GOF-SSA in various water-alcohol solutions.

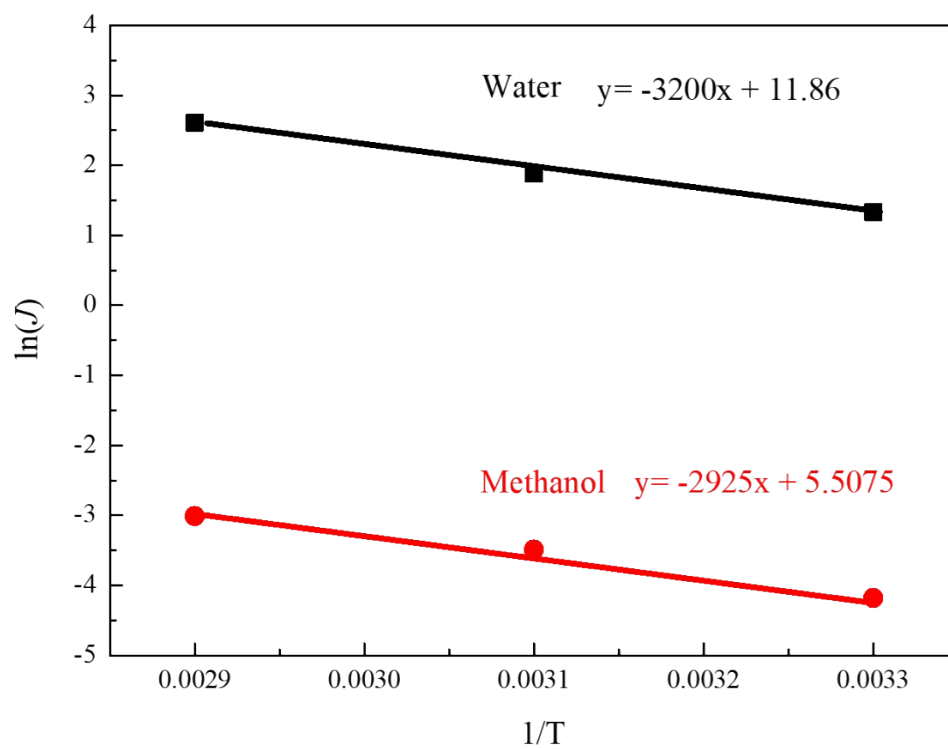
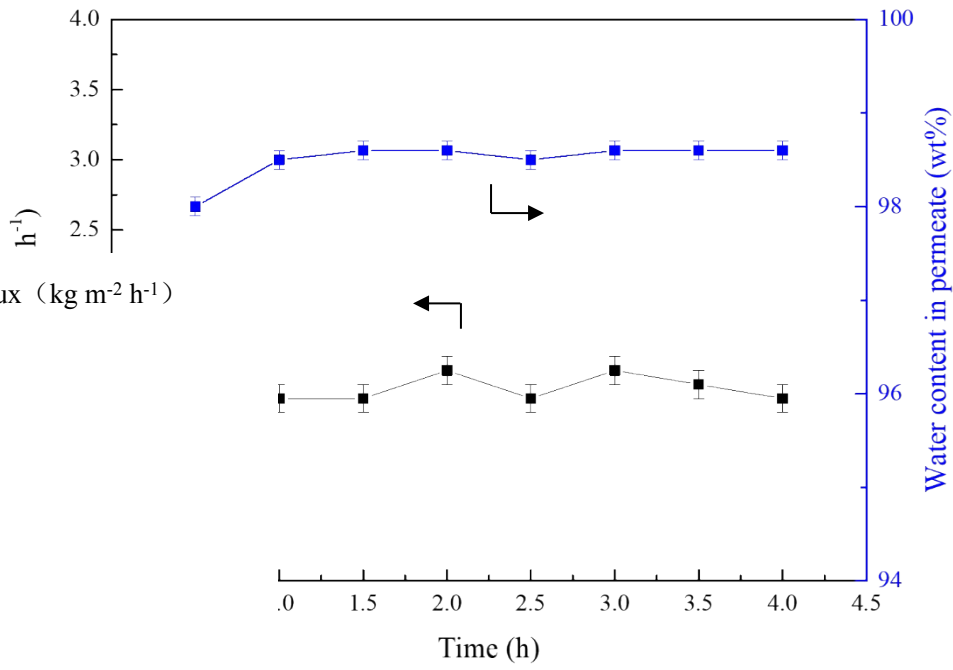


Fig. S19 The Arrhenius plot for water flux and methanol flux.



Dehydration of methanol using GOF-SA membrane.

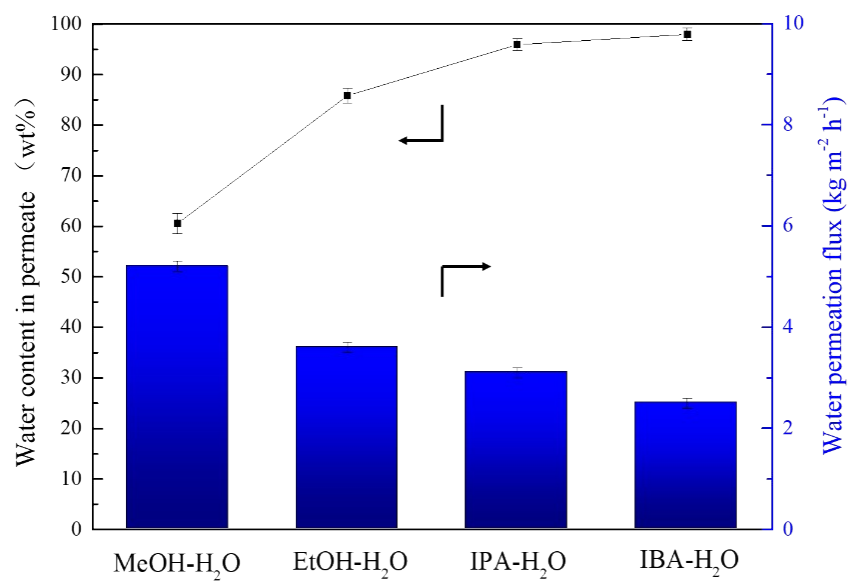


Fig. S21 Dehydration of alcohol using control GO membrane.

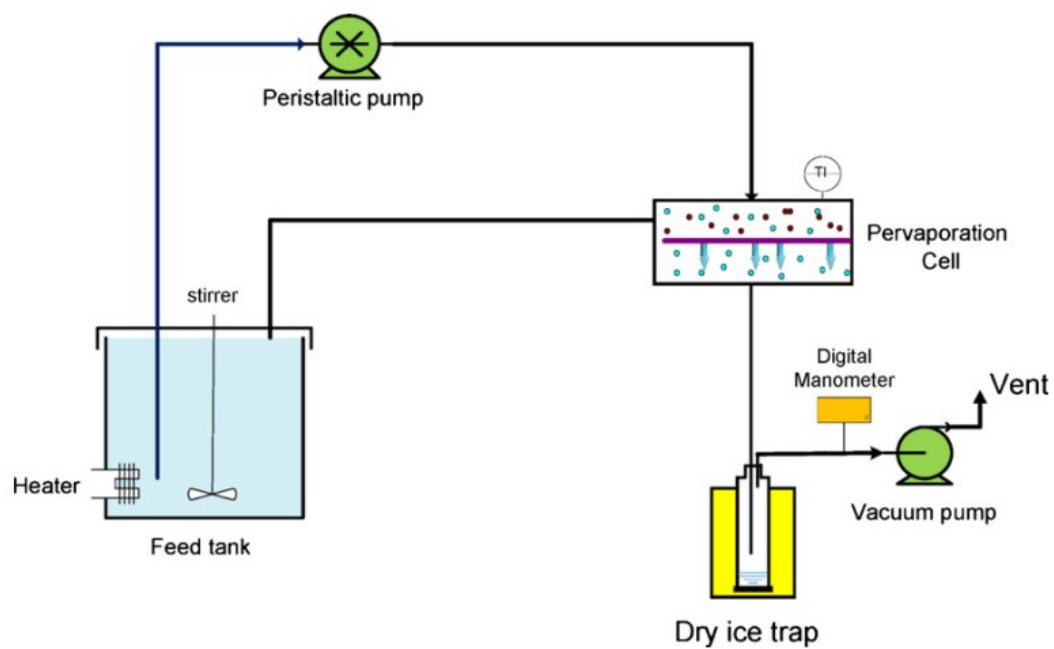


Fig. S22 Schematic drawing of the pervaporation unit.

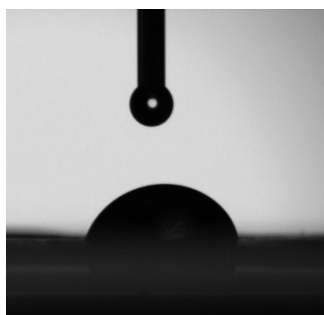


Fig. S23 Water contact angle of the nylon substrate.

Table S1 EDS composition of GOF-SSA in terms of weight percentage (wt%) with standard deviation of 0.1.

Elements	Surface	Cross-section
C	62.3	80.3
O	35.3	17.6
S	2.4	2.1

Table S2 Elemental quantification derived from XPS survey spectra presented as atomic% and atomic ratios (X/C) for GOF-SSA, GOF-SA and control GO membranes. Listed are the mean values with standard deviation.

Sample:	Control GO		GOF-SA		GOF-SSA	
Atomic%	Mean	Std Dev	Mean	Std Dev	Mean	Std Dev
O 1s	29.14	<i>0.35</i>	29.57	<i>0.23</i>	29.54	<i>0.23</i>
C 1s	69.60	<i>0.34</i>	69.09	<i>0.17</i>	68.14	<i>0.17</i>
S 2p	0.21	<i>0.01</i>	0.17	<i>0.01</i>	0.96	<i>0.03</i>
Atomic ratios (X/C)	Mean	Std Dev	Mean	Std Dev	Mean	Std Dev
O 1s	0.419	<i>0.007</i>	0.428	<i>0.004</i>	0.434	<i>0.004</i>
N 1s	0.009	<i>0.000</i>	0.014	<i>0.001</i>	0.018	<i>0.000</i>
C 1s	1.000	<i>0.000</i>	1.000	<i>0.000</i>	1.000	<i>0.000</i>
S 2p	0.003	<i>0.000</i>	0.002	<i>0.000</i>	0.014	<i>0.000</i>
Relative fraction of C, %	Mean	Std Dev	Mean	Std Dev	Mean	Std Dev
C1 - (C=C/C-C/C-H/C-S)	44.73	<i>0.04</i>	47.42	<i>0.36</i>	48.80	<i>0.27</i>
C2 - (C-O-C/C-OH)	46.14	<i>0.51</i>	41.39	<i>0.96</i>	39.81	<i>1.03</i>
C3 - (C=O)	4.40	<i>0.21</i>	3.39	<i>0.42</i>	4.17	<i>0.10</i>
C4 - (O-C=O)	4.74	<i>0.35</i>	7.81	<i>0.18</i>	7.22	<i>0.66</i>
	Mean	Std Dev	Mean	Std Dev	Mean	Std Dev
C2/C1	1.032	<i>0.010</i>	0.873	<i>0.027</i>	0.816	<i>0.026</i>
C4/C1	0.106	<i>0.008</i>	0.165	<i>0.002</i>	0.148	<i>0.013</i>